# Dielectric and Acoustic Properties with a Single Laboratory Instrument

Matthew Josh
CSIRO Energy, 26 Dick Perry ave, Kensington, WA 6151, Australia

*This paper was prepared for presentation at the International Symposium of the Society of Core Analysts held in Vienna, Austria, 27 August – 1 September 2017*

## ABSTRACT

Electrical and acoustic petrophysical models derived from laboratory testing of rock samples are two of the principal methods for estimating the key reservoir properties (porosity, fluid permeability, fluid type, saturation and mineralogy) from borehole logs. The current generation of multi-frequency dielectric logging tools, which have appeared in the petroleum industry in the last decade, have led to a resurgence in all aspects of rock electrical properties, not limited to simply the low frequency conductivity, but including both real and imaginary components of dielectric permittivity and covering a broad spectrum of frequencies. This is due partly to the desire to use dielectric mixing rules to determine rock saturation, which is more easily achieved at approximately 1 GHz, and because dielectric permittivity strongly correlates with specific surface area and cation exchange capacity in the vicinity of 20 – 100 MHz. A novel laboratory petrophysical instrument has been developed which integrates both swept frequency dielectric analysis with P-wave velocity, on thin samples typically 8 mm thick, so that a single small sample can be machined and hydrated then analysed to provide both properties simultaneously. The instrument was able to resolve P-wave transit time in a Teflon sample less than 1 mm thickness, and was further validated with a number of non-porous engineering materials including sapphire, plexiglass and quartz. When applied to porous geological samples including Fontainebleau sandstone and Berea sandstone the real relative dielectric permittivity increased from approximately 4 when the sample was baked dry to approximately 6.8 (Fontainebleau) and 12 (Berea) when the sample was vacuum saturated with DI water. Simultaneously the P-wave velocity in both sandstones was higher in the saturated case.

## INTRODUCTION

Acoustic and dielectric properties are two of the fundamental rock parameters which are exploited by the petroleum industry for evaluating reservoirs. During exploration, acoustic properties are integral to the application of surface seismic and likewise electrical properties are integral to CSEM. These same petrophysical parameters are also used during drilling and production to provide more targeted information about the extent of the reserves in-place and provide input to production related decision making. Clearly each of these activities are founded on a substantial background in laboratory based rock properties determination, which is used to create the rock physics models which relate the ultimate reservoir parameters: porosity, mineralogy, fluid permeability, saturation and fluid type to the petrophysical properties which can be measured from the surface or borehole. Numerous examples of this can be found in the petroleum industry and related literature **(Archie, 1941; Mazzagatti et al., 1983; Myers, 1991; Seleznev et al., 2011; Sen and Chew, 1983, Shen et al., 1987)**. The most widely used and recognised example is Archie's law,

$$R_t = a\phi^{-m} S_w^{-n} R_w \qquad (1)$$

which relates the resistivity of the rock ($R_t$) to the porosity ($\phi$), saturation ($S_w$), tortuosity factor (a) and brine resistivity ($R_w$) via a pair of simple exponents (Archie parameters, *m*, the cementation exponent and n, the saturation exponent), which need to be evaluated for the particular field or formation being investigated **(Ellis and Singer, 2007)**. Archie's law has been a staple of the petroleum industry ever since its publication. However, difficulties in estimating porosity from resistivity created by variations in formation salinity, have led to later advancements in high frequency dielectric logging, because dielectric permittivity is less affected by salinity. This has been complimented by alternative dielectric mixing models such as the complex refractive index method (CRIM, **Birchak et al., 1974):**

$$\sqrt{\varepsilon_{eff}} = \phi S_w \sqrt{\varepsilon_{rw}} + \phi(1 - S_w)\sqrt{\varepsilon_h} + (1-\phi)\sqrt{\varepsilon_{ma}} \qquad (2)$$

where $\varepsilon_{eff}$ is the effective dielectric permittivity of the formation and $\varepsilon_{ma}$ and $\varepsilon_{rw}$ are the rock matrix and pore fluid dielectric permittivities respectively and $\varepsilon_h$ is the dielectric permittivity of gas. CRIM is often used with the current generation of high frequency dielectric logging tools to quantify, porosity and pore fluid type **(Seleznev et al., 2011).** Similarly, the rock acoustic properties, including the compressional (primary or P-) wave **(Gassmann, 1951)** are derived from elastic theory,

$$V_p = \sqrt{\frac{K + \frac{4}{3}\mu}{\rho}} \qquad (3)$$

where P-wave velocity, $V_p$, is related to the bulk modulus (K), shear modulus ($\mu$) and the rock bulk density ($\rho$) and each of these properties is also affected by the porosity, pore fluid type and saturation. Rocks present a range of challenges that are less significant in other fields of materials research, even when it is possible to obtain intact, representative and reasonably homogenous samples. For example engineering materials such as glass and polymers are often characterised by their consistency regardless of their origin and do not change significantly with time or other regular laboratory environmental factors. Rocks however, continually rehydrate and equilibrate with humidity and temperature and one of the challenges which confronts laboratory petrophysics is the consistency of any given sample during multiphysics tests. This is compounded by the requirement of specific sample geometries for different tests. A relatively short (~ < 10 mm) sample used for parallel plate dielectric analysis is preferred to avoid fringing field capacitance compared with the relatively long (~ 60 mm) sample used for acoustic analysis chosen to insure adequate wavelengths within the sample and achieve acceptable resolution.

A new laboratory instrument is presented, which addresses the requirement to test rock samples with consistent hydration and under stable and repeatable laboratory conditions by achieving P-wave velocity measurement and dielectric measurement simultaneously on a short sample of < 10 mm. This was achieved by the design and manufacturing of the world's first integrated dielectric electrode assembly containing piezo-transducers, with a frequency high enough to achieve satisfactory acoustic analysis in a < 10 mm sample. The instrument has been validated using a number of engineering materials and rock samples.

## INSTRUMENT PRINCIPLES

The instrument was developed from the principles of a regular parallel plate capacitor which is commonly used in dielectric standards **(Von Hippel, 1954)** and has been used regularly in laboratory petrophysics **(Keysight 5989-2589EN, Mazzagatti et al., 1983; Shen et al., 1987)**. This style of instrument has the advantage of a relatively large volume of investigation compared with end-loaded coaxial transmission line instruments **(Stuchly and Stuchly, 1980)** and a convenient sample geometry compared with through-loaded airline instruments **(Nicholson and Ross, 1970; Keysight App Note 5989-2589EN).** A parallel plate dielectric instrument can perform beyond 100 MHz, which covers much of the frequency range of the current state of the art in multi-frequency dielectric logging tools. Parallel plate dielectric cells produce a uniform and parallel electric field which provides the advantage of allowing anisotropy analysis, which is not available with either end-loaded or airline coaxial measurement. They use large electrode surfaces which are similar and compatible with acoustic platen geometries and this has made possible the integration of piezo-ceramic componentry to create a fully integrated dielectric and acoustic platen (Figure 1a), which allows both measurements to be made simultaneously. The instrument is attached to two separate external circuits (highlighted in orange and blue, Figure 1a) to achieve the simultaneous measurement. An impedance analyser (Agilent 4294a, Figure 1b) determines the equivalent parallel capacitance ($C_p$) and resistance ($R_p$) (Figure 1c) between the guarded and unguarded electrodes which is then converted into the real and imaginary dielectric permittivity and conductivity via:

$$\varepsilon^* = \varepsilon_0 \times \varepsilon_r^* = \varepsilon_0 \times (\varepsilon'_r + j\varepsilon''_r) \qquad (4)$$

$$\varepsilon'_r = \frac{C_p d}{\varepsilon_0 A} \qquad (5)$$

$$\sigma_{equivalent} = \frac{d}{R_p A} \qquad (6)$$

$$\varepsilon''_{r\,equivalent} = \frac{d}{2 \times \pi \times f \times \varepsilon_0 \times R_p \times A} \qquad (7)$$

where A, is the area of the capacitor plates, d is the thickness of the sample, $\varepsilon_0$ is the permittivity of free space, $\varepsilon^*_r$ is the complex relative permittivity of the sample and σ is the conductivity of the sample.

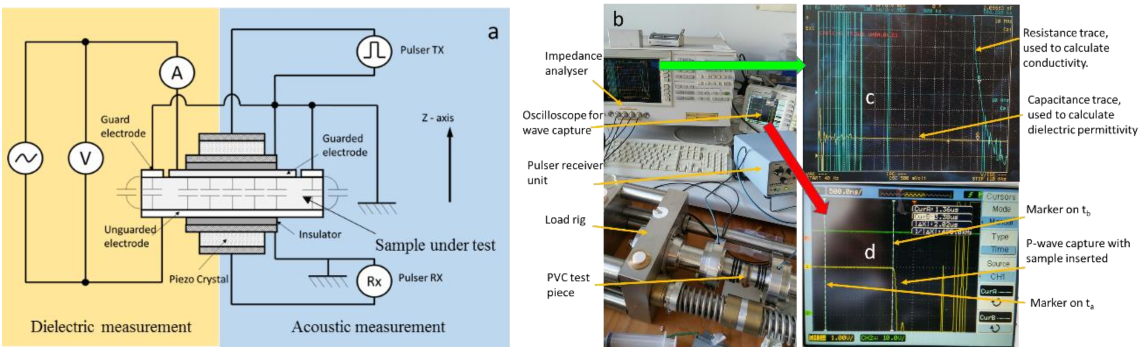

Figure 1: a) The circuit schematic of the instrument including both external circuits (orange background) the conventional three terminal connected parallel plate dielectric cell and (blue background) the conventional pulser-receiver configuration which drives and detects signal through the matched piezo-crystal pair. The P-wave propagates in the same direction as the electric field is oriented. b) The instrument can generate both electrical and acoustic data sets simultaneously. A polymer sample (grey PVC) is inserted into the instrument in the foreground and the two traces visible on two separate instruments are being saved simultaneously and provided in the breakout data. c) the dielectric trace and d) the acoustic trace.

The instrument is simultaneously connected to an ultrasonic pulser receiver unit (Olympus 5077PR, Figure 1b), which is used to drive the piezo-ceramic crystals housed within the transducer platens. A high voltage, typically 100 – 400 V, drives one of the transducer pairs whilst the other is connected through the pulser-receiver unit to an oscilloscope to capture the received waveform (Figure 1d).

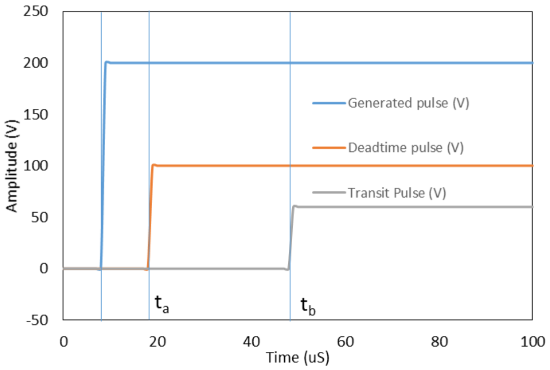

Figure 2: Sketch of the captured acoustic waveforms. (blue) The generated (transmitted) pulse, (orange) the deadtime pulse detected at the receiver (at time $t_a$) when the transducers are connected together without a sample. (grey) Transit pulse detected at the receiver (at time $t_b$) when the sample is inserted between the transducers.

Separate calibration processes are required for the two instrument measurement functions. The dielectric function is calibrated using short, open and load test pieces to remove the series and parallel stray impedances of the cell when connected to the impedance analyser. The acoustic measurement is calibrated by directly coupling the transducers together and capturing a waveform of the so-called *deadtime* pulse and recording the deadtime (Figure 2), $t_a$, which is related to cable lengths, transducer geometry and internal electronics of the pulser-receiver unit. Then the sample under test is inserted between the transducers and a new waveform is captured at time $t_b$. The transit time of the pulse through the sample is calculated along with the velocity (P-wave) and the number of wavelengths interacting with the sample using,

$$Transit\ time = t_b - t_a \qquad (8)$$

$$P - wave\, velocity = \frac{d}{Transit\ time} = \frac{d}{t_b - t_a} \qquad (9)$$

$$Number\ of\ wavelengths = n = f \times (t_b - t_a) \qquad (10)$$

where $f$, is the transducer frequency and d is the thickness. Accepted rules of thumb in acoustic analysis **(ASTM Designation D2845 – 00, 2000)** dictate that approximately 10 wavelengths should interact with the sample to allow sufficient resolution of the P-wave arrival "picks" and typically for a $f$ = 1 MHz instrument the preferred minimum sample length is approximately 20 – 30 mm. For this instrument dielectric analysis requires a sample that is less than 10 mm thick and so a piezo-crystal operating at $f$ = 4.6 MHz (nominally 4.0 MHz, but measured otherwise) was used to create a shorter wavelength. The dielectric–acoustic platens are mounted into a large stainless steel housing which can be inserted into a uniaxial load cell. This ensures that a reliable acoustic connection is made between the sample and the platens and that series impedance is not affected by an airgap. Samples must cover no less than diameter 25 mm, determined by the diameter of the guarded electrode. The sample can have any shape, such as a rectangular tile or a rough cut piece of rock from core, so long as it has precision cut parallel faces with a tolerance of 30 µm determined by a small amount of play built into the instrument. Many engineering materials such as glass are already manufactured to these specifications and need only be prepared into a sample small enough to be manageable Table 1.

## RESULTS

A selection of samples were prepared and measured to validate and demonstrate the instrument. These included *polymers*, Plexiglass (Perspex/Acrylic or PMMA) and Teflon in multiple thicknesses; *ceramics*, quartz and sapphire, which has an ultra-high P-wave velocity; *metals*, aluminium 6061-T6 and stainless steel 316, which were not useful as dielectric standards, but have well accepted acoustic properties; and *geological samples* Fontainebleau sandstone and Berea sandstone in different states of saturation.

Table 1: A table of engineering materials and geological samples investigated in this study, included a number of common reference materials, glasses and polymers along with two selected geological materials in different states of saturation. The metal samples are too conductive for the instruments range of sensitivity.

| | Sample thickness (mm) | P-wave travel time (nS) | P-wave velocity, Vp (m/s) | Number of wavelengths | Capacitance at 10 MHz (pF) | Resistance at 10 MHz (Ω) | Real relative dielectric permittivity, εr at 10 MHz | Conductivity at 10 MHz (S/m) |
|---|---|---|---|---|---|---|---|---|
| TeflonA | 0.25 | 160 | 1563 | 0.736 | 26.028 | 4.53E+00 | 2.03 | 1.52E-13 |
| TeflonB | 0.50 | 360 | 1389 | 1.656 | 12.897 | 5.04E+00 | 2.01 | 2.73E-13 |
| TeflonC | 1.99 | 1400 | 1421 | 6.440 | 3.429 | 2.13E+01 | 2.12 | 2.57E-13 |
| TeflonD | 4.99 | 3560 | 1402 | 16.376 | 1.349 | 1.81E+02 | 2.10 | 7.60E-14 |
| PlexiglassPerspex | 4.88 | 180 | 2711 | 8.280 | 1.82 | 7.23E+05 | 2.76 | 1.86E-05 |
| C-cut Sapphire | 5.25 | 460 | 11413 | 2.116 | 7.56 | 4.67E+05 | 12.35 | 3.10E-05 |
| Quartz | 3.19 | 520 | 6135 | 2.392 | 3.98 | 1.59E+06 | 3.96 | 5.52E-06 |
| Aluminium (6061-T6) | 4.98 | 820 | 6073 | 3.772 | N/A | Very Low | N/A | Very High |
| Stainless Steel (316) | 5.00 | 900 | 5556 | 4.140 | N/A | Very Low | N/A | Very High |
| Dry Berea | 7.70 | 2.84 | 2711 | 13.064 | 1.83 | 7.58E+04 | 4.38 | 2.80E-04 |
| Wet Berea | 7.70 | 2.38 | 3235 | 10.948 | 6.36 | 2.36E+03 | 15.24 | 8.98E-03 |
| Dry Fontainebleau | 9.84 | 3.74 | 2631 | 17.204 | 1.31 | 1.65E+06 | 4.02 | 1.65E-05 |
| Wet Fontainebleau | 9.84 | 2.30 | 4278 | 10.580 | 2.36 | 3.57E+04 | 7.21 | 7.60E-04 |

For all of the geological samples tested, more than 10 wavelengths interacted with the sample. In thin polymer samples (including the 0.25 mm thick Teflon) or in ultra-high speed materials such as sapphire, it is evident that the number of wavelengths interacting with the sample was substantially less than 10, however these materials do not fall within the intended scope-of-purpose of the instrument. As a comparison, the measured P-wave velocity of the plexiglass is 2711 m/s compared with the published value of 2750 m/s **(www.signal-processing.com/table.php),** and C-cut sapphire measures 11413 m/s compared with published values of 11100 m/s **(www.signal-processing.com/table.php)** and 11913 m/s **(Adavnced NDT)**. Measured and published values for P-wave velocity are consistent for the entire sample collection. The P-wave velocity in Berea sandstone has increased from 2711 m/s to 3235 m/s from dry to saturated, compared with Fontainebleau sandstone increasing from 2631 to 4278 m/s. i.e. Fontainebleau sandstone demonstrates a much bigger change with saturation even though it is less than ½ as porous. The Berea sandstone had a porosity of $\phi_{pycn}$ = 20.5 % from helium pycnometery and $\phi_{mass}$ = 19.60 % from the vacuum saturated mass. The Fontainebleau sandstone had a porosity of $\phi_{pycn}$ = 8.80 % from helium pycnometery and $\phi_{mass}$ = 8.85 % from vacuum saturated mass. The complex dielectric permittivity in the geological samples significantly increased after they were saturated. The measured complex relative permittivity of Fontainebleau sandstone increased from $\varepsilon^*_r = 4.072 + 0.0596j$ to $\varepsilon^*_r = 6.865 + 0.1746j$ at 100 MHz. Using values determined in the laboratory, $\varepsilon^*_{rw} = 81 + 0.467j$ (deionised, DI, water), $\varepsilon^*_{ma} = 3.96 + 0.0204j$ (quartz sample provided) and $\varepsilon^*_h = 1$ (air), CRIM estimates a sample complex relative permittivity of $\varepsilon^*_{eff} = 6.796 + 0.0363j$ which increases to $\varepsilon^*_{eff} = 6.797 + 0.268j$ if $\varepsilon^*_{rw} = 81 + 5.9j$ (i.e. brine is used rather than DI). This would be consistent with a formation brine of approximately 0.1 g/l NaCl. Measured Berea has increased from $\varepsilon^*_r = 4.033 + 0.2308j$ to $\varepsilon^*_r = 12.00+2.661j$ at 100 MHz where CRIM estimates $\varepsilon^*_{eff} = 11.744 + 0.0644j$ using DI water and $\varepsilon^*_{eff} = 11.864 + 2.661j$ when $\varepsilon^*_{rw} = 81 + 34.05j$, which is consistent with a formation brine of approximately 0.5g/l. These small increases in water imaginary permittivity can be accounted for by a small amount of salt residue within the rock samples. The increase observed in the real relative dielectric permittivity of the dry to saturated sandstones is nearly perfectly estimated by CRIM indicating there is no evidence for interaction between the constituents, which would be more common at lower frequencies or if clay content was significant.

The transit time through the different thicknesses of Teflon sample are perfectly correlated with the thickness of the sample (Figure 3) consistent with equation 9 and a gradient corresponding to a P-wave velocity of 1372 m/s, which matches published values of 1400 m/s **(NPL)** and 1372 m/s **(Adv. NDT).** More surprising is that the 0.25 mm thickness sample is resolvable from the 0.5 mm thick sample and both are consistent with the global trend which has a correlation coefficient of $R^2 = 0.9999$. This suggests that although the sample is extremely thin for the frequency of measurement (i.e. less than 1 wavelength within the sample) the resolution appears to be sufficient, although this is not recommended **(ASTM Designation D2845 – 00, 2000)**.

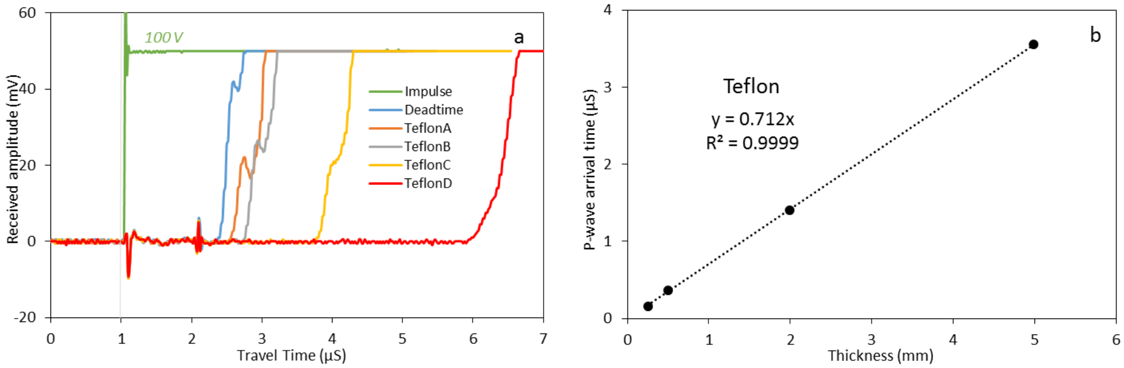

Figure 3: a) P-wave captures through the 4 different Teflon samples with different thicknesses. The waveforms are overlaid along with the driving pulse and the deadtime pulse created when no sample is inserted between the platens. The arrival time of the front edge of the P-wave increases with the thickness of the sample. b) The arrival time of the P-wave correlates ($R^2 = 0.9999$) nearly perfectly with the thickness of the Teflon sample; in addition, the 0.25 mm and 0.5 mm thick samples are consistent with the thicker samples indicating that thin samples do not appear to be a problem for this instrument.

The capacitance of the Teflon loaded cell also varies inversely with the thickness of the sample (Table 1), exhibiting a correlation coefficient of $R^2 = 0.9999$, which is consistent with equation 5 above.

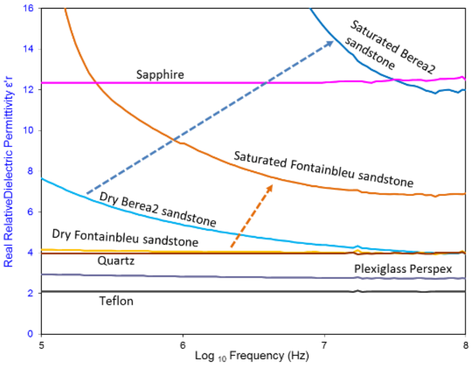

Figure 4: Dielectric frequency response of the polymers, ceramics and saturated geological samples. The geological samples both increase in dielectric permittivity after being saturated. Dry Fontainebleau sandstone has an almost identical dielectric permittivity to that of a synthetic single crystalline quartz sample.

The polymers and ceramics that were measured generally exhibit no change in dielectric permittivity as the frequency is increased (Figure 4), whereas the geological samples generally exhibit a reduction in dielectric permittivity with increasing frequency i.e. they are dispersive. This is one reason why *"multi-frequency"* is the state of the art in dielectric logging in the petroleum industry. Dielectric permittivity of clay bearing rocks is largely determined by the cation exchange capacity **(Myers, 1991)**, and subsequent investigations **(Leung and Steiger, 1992; Josh, 2014),** demonstrate that the three properties CEC, SSA and dielectric permittivity, usually vary together, in an essentially linear relationship with as much as 90 % correlation. However, this correlation generally appears to weaken slightly as the frequency is increased above 100 MHz because the longer scale polarisation mechanisms begin to "turn-off" **(Guéguen and Palciauskas, 1994; Sen and Chew, 1983)**. Polymers and ceramics, however do not exhibit this phenomenon, they are mostly nondispersive. For example sapphire has a real dielectric permittivity of $\varepsilon'_r$ = ~12.35 **(c.f. 11.1 Harman et al., 1994)** and quartz $\varepsilon'_r$ = ~3.95 **(c.f 3.78, Von Hippel, 1954)**. Plexiglass has a real dielectric permittivity of $\varepsilon'_r$ = ~2.83 at 1 MHz which reduces to $\varepsilon'_r$ = 2.74 at 100 MHz **(c.f. 2.76 at 1 MHz and ~2.69 at 100 MHz, Von Hippel, 1954)** and is more dispersive than many other polymers. Fontainebleau sandstone is a nearly pure quartz content, low porosity sandstone, consisting of very fine quartz grains highly cemented together. It's dry state dielectric properties nearly perfectly match that of quartz, however the dielectric permittivity of the Fontainebleau sandstone is very slightly dispersive, probably because of a surficial contribution caused by a small content of water incorporated into the quartz cement **(French and Worden, 2013)** and possibly additional water adsorbed from the atmosphere.

## CONCLUSION

The use of electrical and acoustic logging in the petroleum industry has always required corresponding laboratory measurements on core samples to provide calibration and to establish the essential physical models (e.g. Archie's Law). The appraisal of conventional and unconventional reservoirs relies on proper quantification of basic rock parameters such as mineralogy, organic matter content, porosity, fluid permeability and fluid type and saturation, which are only indirectly determined from the downhole measurements. Well calibrated cross-property relationships then allow borehole measurements such as electrical properties including dielectric permittivity; acoustic properties and other physical measurement, to be used to estimate the properties of interest.

The development of a combined dielectric and acoustic instrument allows both permittivity and velocity to be measured simultaneously on a single sample, so that the data sets have guaranteed equivalence/correspondence. This was achieved through the design, development and testing of a novel electrical and acoustic platen customised to the short samples that are typically used in dielectric analysis. The instrument has been demonstrated successfully and reproduces the published values for a range of engineering samples, polymers and ceramics. It has also been shown to achieve consistent results on well characterised geological sample standards including Fontainebleau and Berea sandstones.

## ACKNOWLEDGEMENTS

I would like to acknowledge Stuart Dahl, Tony Siggins, Rod Banks and Greg Lupton for instrumentation and componentry, Maxim Lebedev, Joel Sarout, Alexy Yurikov and Claudio Delle Piane, Wayne Murray, Dave Walton for technical assistance. David Dewhurst, Tobias Müller, Marina Pervukhina, Ben Clennell and Emma Josh, for editing.

## REFERENCES

Archie, G. E., 1941, The electrical resistivity log as an aid in determining some reservoir characteristics, Trans. AIME, vol. 146, October.

ASTM Designation D2845 – 00, 2000, Standard test method for laboratory determination if pulse velocities and ultrasonic elastic constants of rock.

Birchak, J. R., C. G. Gardner, J. E. Hipp and J. M. Victor, 1974, High dielectric constant microwave probes for sensing soil moisture: Proceedings of the IE, vol.62, no.1, pp.93,98, January. doi: 10.1109/PROC.1974.9388.

Ellis, D. V. and J. M. Singer, 2007, Well Logging for Earth Scientists, Springer, The Netherlands.

French, M. W. and R. H. Worden, 2013, Orientation of microcrystalline quartz in the Fontainebleau formation, Paris basin and why it preserves porosity, Sedimentary geology, vol. 284 – 285, pp. 149 – 158.

Gassmann, F., 1951, Über die Elastizität poröser Medien. Viertel. Naturforsch. Ges. Zürich, vol. 96, pp. 1 – 23.

Guéguen, Y., and Palciauskas, V., 1994, Introduction to the Physics of Rocks, Princeton University Press, 392 pp.

Harman, A. K., S. Ninomiya, and S. Adachi, (1994). Optical constants of sapphire (alpha-Al2O3) single crystals. Journal of Applied Physics. vol. 76, no. 12, pp. 8032–8036.

Josh, M., 2014, Dielectric permittivity: A petrophysical parameter for shales, Petrophysics, vol. 55, no. 4, pp 319 – 332, August.

Josh, M., B. Clennell, and T. Siggins, 2009, Practical broadband dielectric measurement of geological samples: 50th SPWLA Ann. Logging Symp., Woodlands Texas, June 21-24.

Keysight App. note 5989-2589EN, Basics of measuring the dielectric properties of materials.

Leung P. K., and R. P. Steiger, 1992, Dielectric constant measurements: A new, rapid method to characterize shale at the wellsite: IADC/SPE Drilling Conference paper no. IADC/SPE 23887, New Orleans, USA. pp. 401-408, February.

Mazzagatti, R. P., D. J. Dowling, J. C. Sims, A. E Bussian and R. S. Simpson, 1983, Laboratory measurement of dielectric constant near 20 MHz, SPE 12097 at the 56th Ann. technical conference and exhibition, San Francisco, October 5-8.

Myers, M. T., 1991, A saturation interpretation model for the dielectric constant of shaly sands: International symposium, Society of Core Analysts: SCA Conference paper number 9118, San Antonio, USA.

Nicholson, A. M. and G. F. Ross, 1970, Measurement of the intrinsic properties of materials by time-domain techniques, IEEE trans. instrumentation and measurement, vol. IM – 19, no. 4, November.

Olympus, 5077PR user’s manual, 2000.

Seleznev, N. V., R. L. Kleinberg, M. M. Herron, M. Machlus, A. E. Pomerantz, S. L.

Sen, P. N. and W. C. Chew, 1983, The frequency dependent dielectric and conductivity response of sedimentary rocks, Journal of microwave power, vol. 18, no. 1, pp 95 – 105.

Shen, L. C., H. Marouni, Y. X. Zhang and X. D Shi, 1987, Analysis of the parallel-disc sample holder for dielectric permittivity measurement, IEEE trans. geoscience and remote sensing, vol. GE – 25, no. 5, September.

Stuchly, M. A. and S. S. Stuchly, 1980, Coaxial line reflection methods for measuring dielectric properties of biological substances at radio and microwave frequencies – A review, IEEE trans. instrumentation and measurement, vol. IM – 29, no. 3, September.

Von Hippel, A. R., 1954, Dielectric Materials and their Applications: The Technology Press of M.I.T., United States of America.